

Supplementary information

**Carbon nanocoils decorated with porous NiCo<sub>2</sub>O<sub>4</sub> nanosheets array as highly efficient  
electrode for supercapacitor**

*Khan Abdul Sammed<sup>1</sup>, Lujun Pan<sup>\*1</sup>, Amjad Farid<sup>1, 2</sup>, Muhammad Javid<sup>1</sup>, Hui Huang<sup>1</sup>, Yongpeng Zhao<sup>1</sup>*

*1 School of Physics, Dalian University of Technology, Dalian, 116024, P.R. of China*

*2 Department of Physics, Government College University Faisalabad, Faisalabad*

*38000,pakistan*

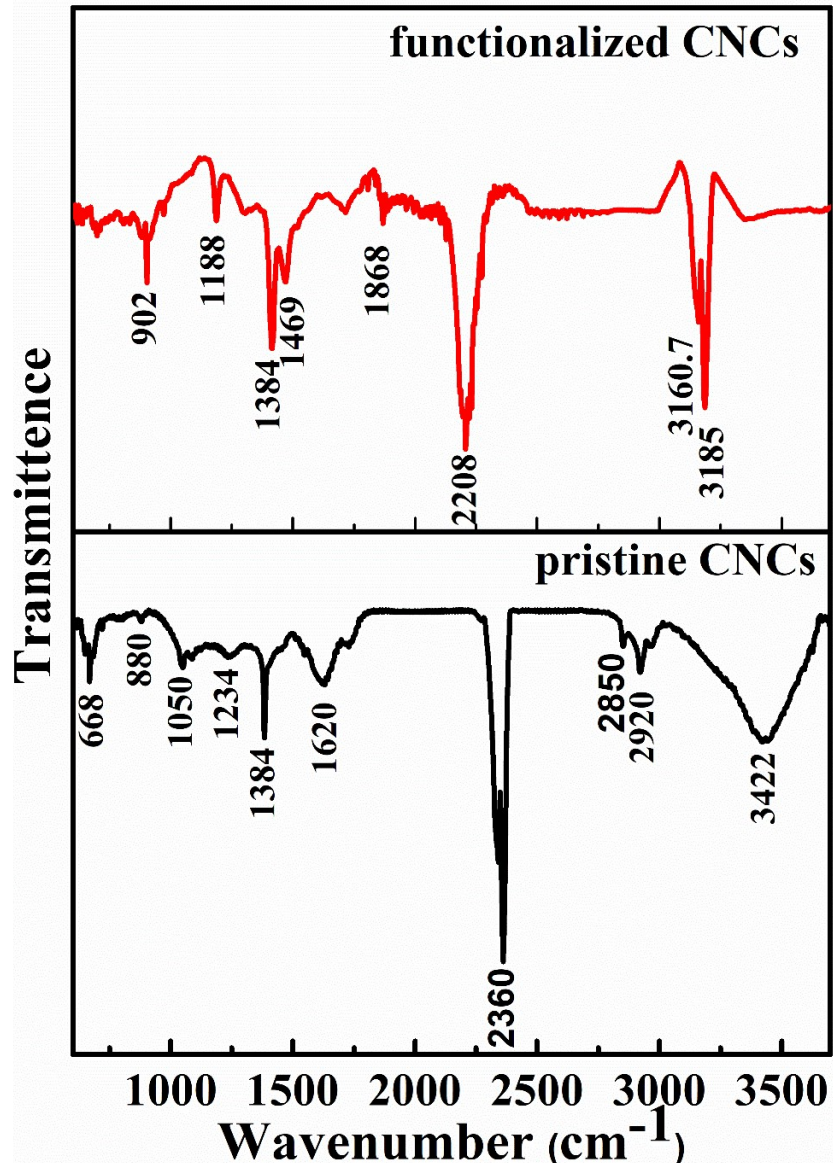


Figure (S 1) FTIR image of pristine CNCs and Functionalized CNCs

The Figure (S 1) shows that the identical bands of vibrations in the FTIR spectrum of functionalized CNCs as compared to pristine CNCs. Which is evident that CNCs are very well oxidized.

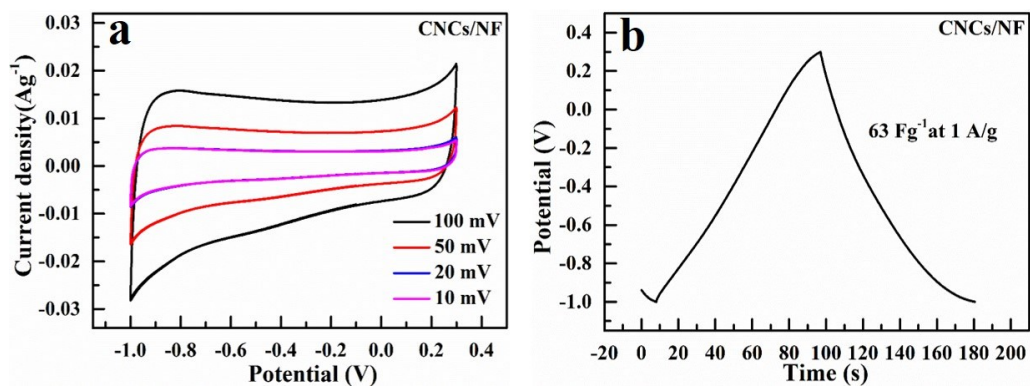


Figure (S2) (a) CV of CNCs/NF, (b) GCD of CNCs/NF

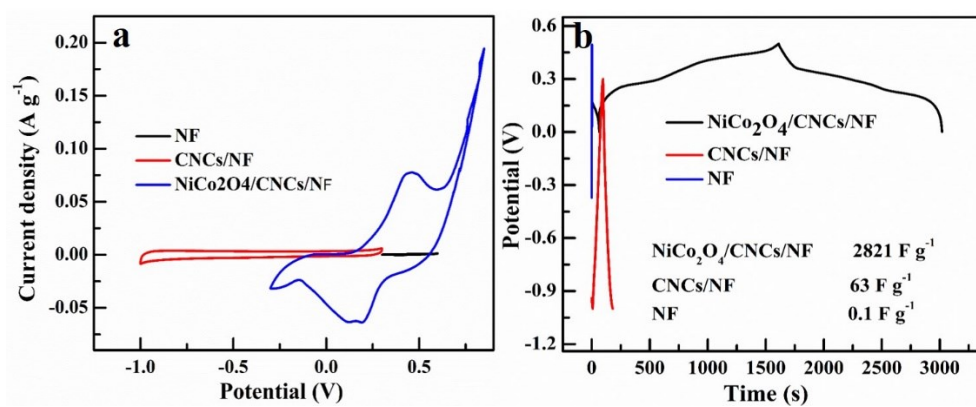


Figure (S3) GCD (a) CV of NF, CNCs/NF and NiCo<sub>2</sub>O<sub>4</sub>/CNCs/NF and (b) GCD of NF, CNCs/NF and NiCo<sub>2</sub>O<sub>4</sub>/CNCs/NF

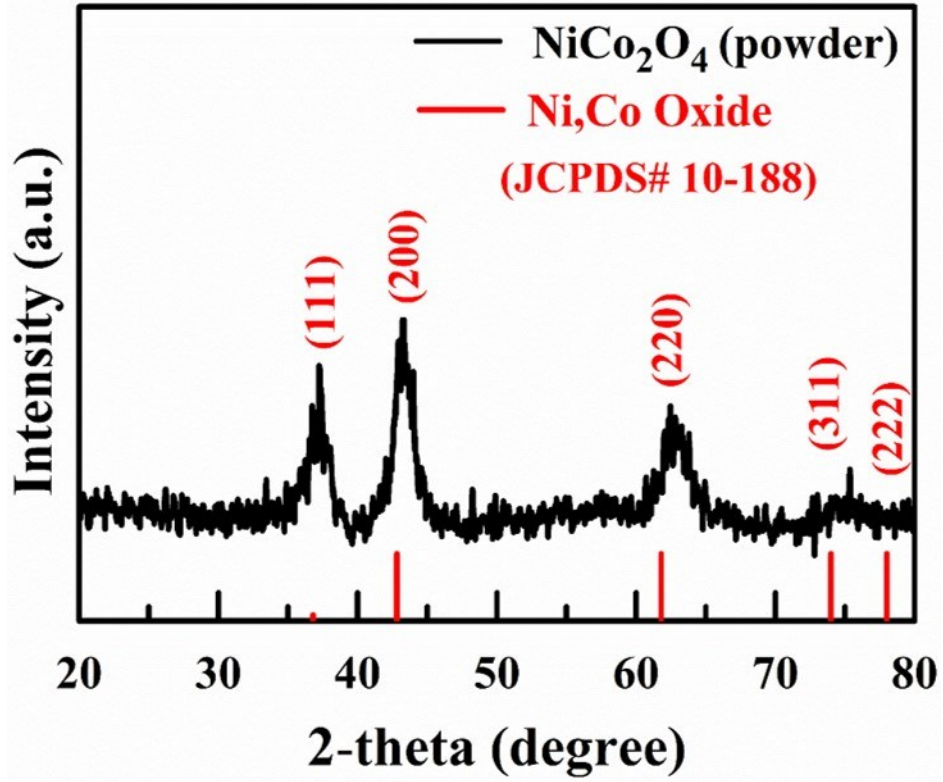


Figure (S4) XRD pattern of NiCo<sub>2</sub>O<sub>4</sub> powder

In order to confirm the formation of NiCo<sub>2</sub>O<sub>4</sub> crystal, XRD technique was employed on as-prepared NiCo<sub>2</sub>O<sub>4</sub> powder. The characteristic XRD spectrum successfully demonstrates that both the Ni and Co oxide phases have been formed as shown in the figure 5. Crystallographic structure of Ni,Co oxide with cubic phase (JCPDS # 10-188) is observed that representing five main characteristic (111), (200), (220), (311) and (222) lattice planes corresponding to the diffraction angles of 36.806<sup>o</sup>, 42.824<sup>o</sup>, 61.799<sup>o</sup>, 73.997<sup>o</sup> and 78.001<sup>o</sup> respectively.

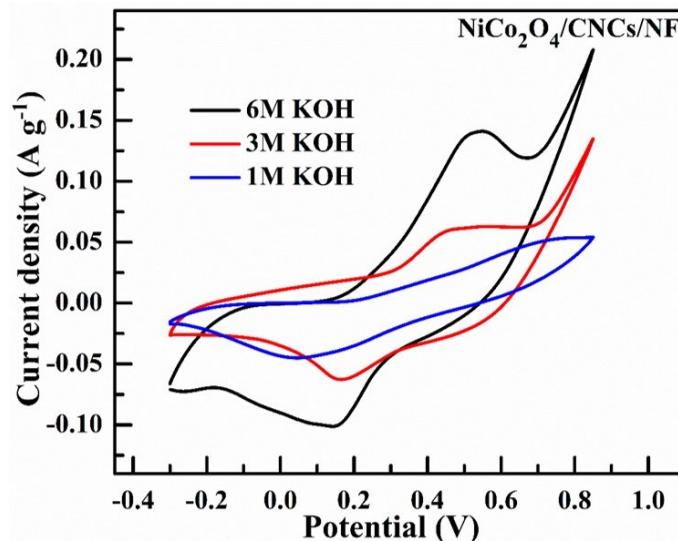


Figure (S5). CV of the NiCo<sub>2</sub>O<sub>4</sub>/CNCs/NF electrode at different concentrations of KOH electrolyte at a scan rate of 50 mV s<sup>-1</sup>

The effect of KOH concentration was investigated by cyclic voltammetry. Fig. (S5) shows the CV curves of the NiCo<sub>2</sub>O<sub>4</sub>/CNCs/NF electrode at the scan rate of 50 mV s<sup>-1</sup> within the potential range of -0.3 to 0.85 V in KOH electrolyte of different concentrations ranging between 1 and 6M KOH. The CVs were more saturated at low electrolyte concentration. When the concentration of KOH was 1.0 M, the CV did not show well resolved anodic peaks. When the concentration of the electrolyte was raised up to 3.0 M, two redox peaks appeared and their intensity was improved in the 6M KOH electrolyte. Clearly, the use of high concentration (6M) KOH benefits the overall electrochemical performance of an electrode. Particularly the redox peak current was largely enhanced with the increase of KOH concentration. This result indicates that the electrochemical redox activity is significantly boosted due to the excessive OH<sup>-</sup> ions<sup>1</sup>.

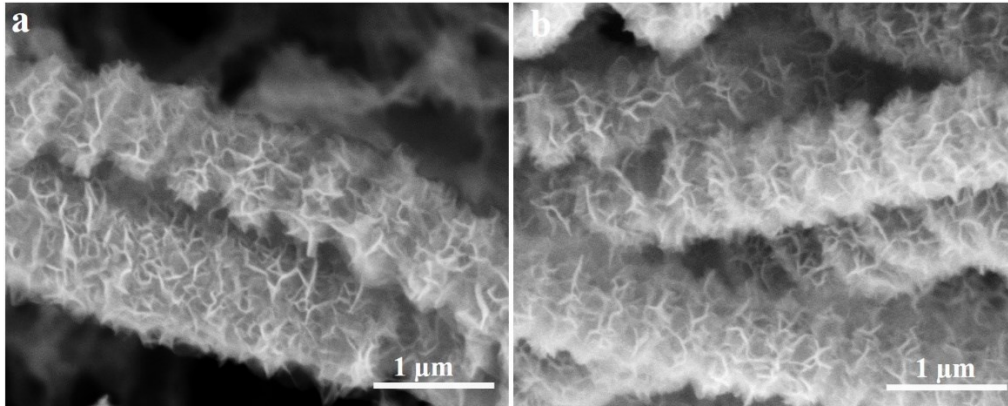


Figure (S6) FE-SEM images of the NiCo<sub>2</sub>O<sub>4</sub>/CNCs/NF composite (a) before and (b) after 3000 charge-discharge cycles

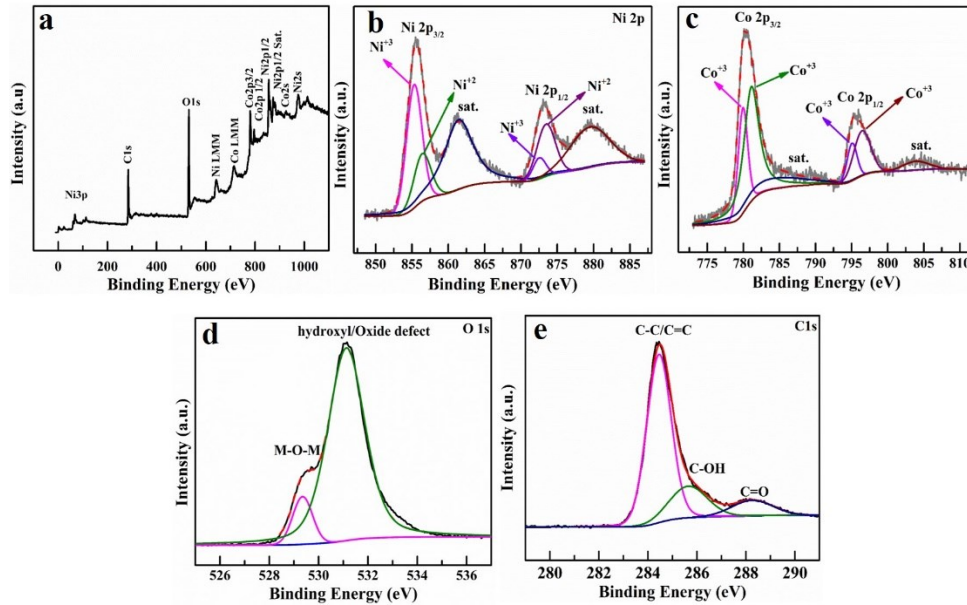


Figure (S7) XPS spectra of NiCo<sub>2</sub>O<sub>4</sub>/CNCs/NF composite (a) survey spectrum, (b) high resolution spectra of O1s, (c) C1s, (d) Ni2p, and (e) Co2p.

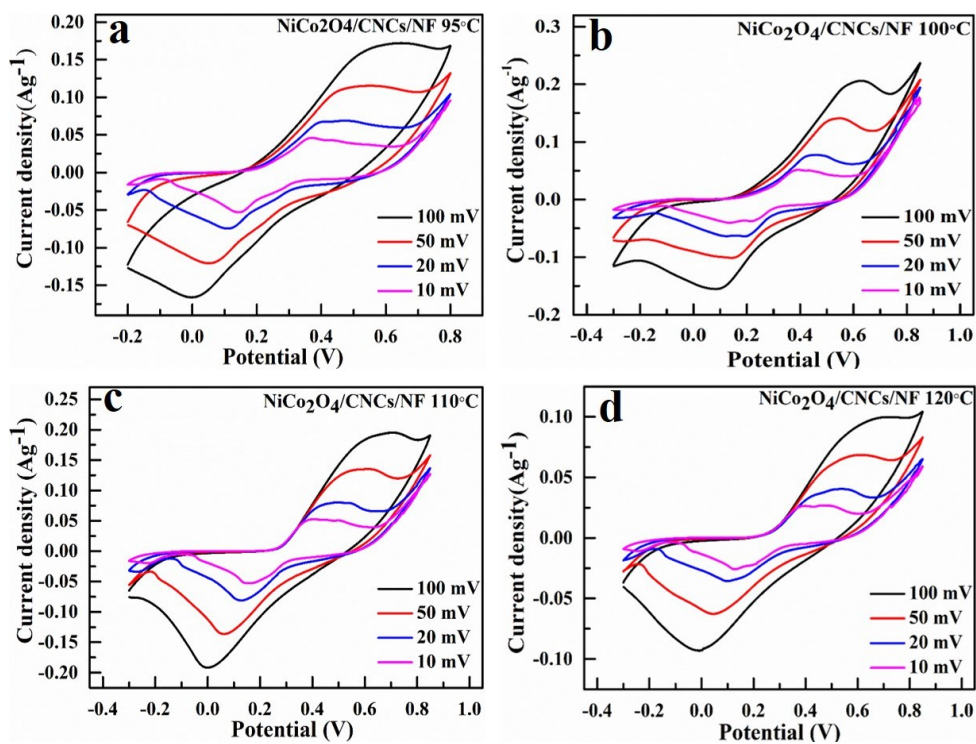


Figure (S8) CV of NiCo<sub>2</sub>O<sub>4</sub>/CNCs/NF composite at (a) 95°C, (b) 100°C, (c) 110°C, (d) 120 °C

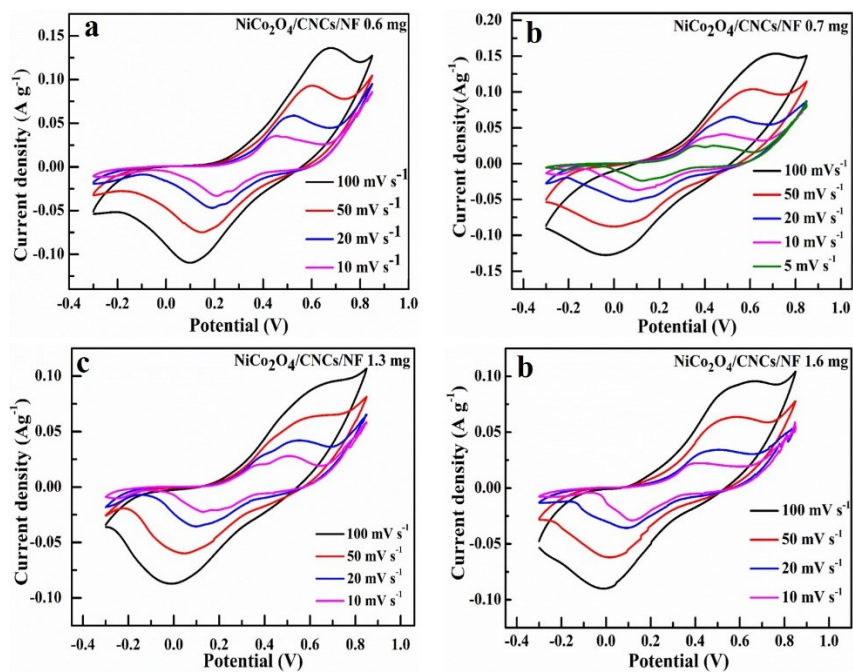


Figure (S9) CV of NiCo<sub>2</sub>O<sub>4</sub>/CNCs/NF composite at (a) 0.6, (b) 0.7, (c) 1.3 and (d) 1.6 mg

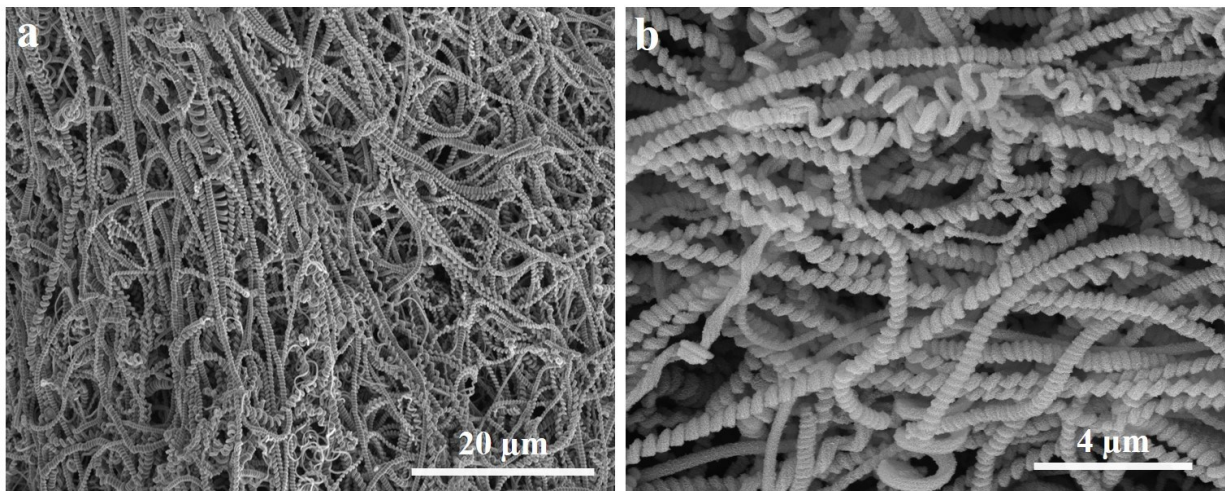


Figure (S10) FE-SEM image of NiCo<sub>2</sub>O<sub>4</sub>/CNCs/NF at (a) low resolution (b) high resolution



Table S1 Comparison of NiCo<sub>2</sub>O<sub>4</sub>/CNCs/NF hybrid with reported literature

Composite electrode	Substrate material	Synthesis method	Specific capacitance	Potential window	Reference
NiCo <sub>2</sub> O <sub>4</sub> /CF	Carbon fabric	Hydrothermal	2658 F g <sup>-1</sup> at 2 A g <sup>-1</sup>	-1 to 0.37	5
NiCo <sub>2</sub> O <sub>4</sub> @NF	Nickel Foam	Combustion	646 F g <sup>-1</sup> at 1A g <sup>-1</sup>	0 to 0.45	6
NiCo <sub>2</sub> O <sub>4</sub> /GF	Graphite Felt	Hydrothermal	2205 F g <sup>-1</sup> at 1 A g <sup>-1</sup>	0 to 0.5	7
NiCo <sub>2</sub> O <sub>4</sub> /3D GF	Graphene foam	Electro deposition	1402 F g <sup>-1</sup> at 1 A g <sup>-1</sup>	0 to 0.5	8
CFs@3D-Ni/NiCo <sub>2</sub> O <sub>4</sub>	3D-Ni modified Carbon fibers	Electro deposition	736 F g <sup>-1</sup> at 1 A g <sup>-1</sup>	0 to 0.5	9
NiCo <sub>2</sub> O <sub>4</sub> /CNT/NF	Carbon nano tube/ Nickel foam	Electro deposition	1533 F g <sup>-1</sup> at 3 A g <sup>-1</sup>	0 to 0.5	10
Ni(OH) <sub>2</sub> @NiCo <sub>2</sub> O <sub>4</sub> /CNT fiber electrode	CNT fibers	Hydrothermal	2397.6 F g <sup>-1</sup> at 5 A g <sup>-1</sup>	0 to 0.45	11
NiCo <sub>2</sub> O <sub>4</sub> @CNFs	carbon nanofibers	Hydrothermal	649 F g <sup>-1</sup> at 3 A g <sup>-1</sup>	-0.2 to 0.6	12
Urchin like NiCo <sub>2</sub> O <sub>4</sub> /rGO	RGo	Solvothermal	672 F g <sup>-1</sup> at 0.5 A g <sup>-1</sup>	0 to 0.5	13
Ni-Co-O@CFP	carbon fiber paper	Hydrothermal	2038 F g <sup>-1</sup> at 1.5 A g <sup>-1</sup>	0 to 0.6	14
NiCo <sub>2</sub> O <sub>4</sub> /GCNF	GCNF	Hydrothermal	1416 F g <sup>-1</sup> at 1 A g <sup>-1</sup>	0 to 0.5	15
(3D rGN/NiCo <sub>2</sub> O <sub>4</sub>	rGN/Cu <sub>2</sub> O film	Chemical	708.3 F g <sup>-1</sup> at 1 A g <sup>-1</sup>	0 to 0.55	16
NF/G/NiCo <sub>2</sub> O <sub>4</sub>	Nickel foam/graphene	Electro deposition	1950 F g <sup>-1</sup> at 7.5A g <sup>-1</sup>	-1 to 0.3	17
NiCo <sub>2</sub> O <sub>4</sub> /CNCs/NF	Carbon Nano coils Nickel Foam	Solvothermal	2821 F g <sup>-1</sup> at 1 A g <sup>-1</sup>	0 to 0.5	Current work

## References:

1. Y. Gao, S. Chen, D. Cao, G. Wang and J. Yin, *Journal of Power Sources*, 2010, **195**, 1757-1760.
2. J. Du, G. Zhou, H. Zhang, C. Cheng, J. Ma, W. Wei, L. Chen and T. Wang, *ACS Applied Materials & Interfaces*, 2013, **5**, 7405-7409.
3. D. R. Kumar, K. R. Prakasha, A. S. Prakash and J.-J. Shim, *Journal of Alloys and Compounds*, 2020, **836**, 155370.
4. X. Zhang, Y. Zheng, W. Zheng, W. Zhao and D. Chen, *Journal of Materials Science*, 2017, **52**, 5179-5187.
5. C. Zhang, T. Kuila, N. H. Kim, S. H. Lee and J. H. Lee, *Carbon*, 2015, **89**, 328-339.
6. H. Li, Z. Feng, H. Che, Y. Liu, Z. Guo, X. Zhang, Z. Zhang, Y. Wang and J. Mu, *Journal of Materials Science: Materials in Electronics*, 2020, **31**, 17879-17891.
7. X. Li, W. Sun, L. Wang, Y. Qi, T. Guo, X. Zhao and X. Yan, *RSC Advances*, 2015, **5**, 7976-7985.
8. H. He, X. Yang, L. Wang, X. Zhang, X. Li and W. Lü, *Chemistry – A European Journal*, 2020, **26**, 17212-17221.
9. A. G. El-Deen, M. Hussein El-Shafei, A. Hessein, A. H. Hassanin, N. M. Shaalan and A. A. El-Moneim, *Nanotechnology*, 2020, **31**, 365404.
10. M. Isacfranklin, G. Ravi, R. Yuvakkumar, P. Kumar, D. Velauthapillai, B. Saravanakumar, M. Thambidurai and C. Dang, *Ceramics International*, 2020, **46**, 16291-16297.
11. M. S. Javed, M. K. Aslam, S. Asim, S. Batool, M. Idrees, S. Hussain, S. S. A. Shah, M. Saleem, W. Mai and C. Hu, *Electrochimica Acta*, 2020, **349**, 136384.
12. G. Yang and S.-J. Park, *Journal of Alloys and Compounds*, 2020, **835**, 155270.
13. Y. Zhou, Z. Huang, H. Liao, J. Li, H. Wang and Y. Wang, *Applied Surface Science*, 2020, **534**, 147598.
14. V. H. Nguyen and J.-J. Shim, *Journal of Power Sources*, 2015, **273**, 110-117.